# STATIC ANALYSIS OF ISOTROPIC & ORTHOTROPIC PLATES WITH CENTRAL CUTOUT SUBJECTED TO EQUI-BIAXIAL LOADING

**KANAK KALITA, ABHIK KUMAR BANERJEE**

**Abstract:** In the present work a study on deflection and stress concentration of thin rectangular plates with internal cutout subjected to biaxial loading is conducted. This study involves obtaining variation in deflection pattern and stress concentration factor by using finite element method. Eight node shell element with 6 degrees of freedom at each node is used in this analysis. The effect of shape of cutout, cutout dimension by plate side length ratio (d/B or b/B), boundary conditions and effect of material properties is observed. The results of the analyzed models are presented here in graphical form. A popular finite element package ANSYS is used for the analysis.

**Keywords:** *Deflection, Finite Element Method,Biaxial Loading, Internal Cutout, Stress.*

**Introduction:** In engineering design, Stress Concentration Factor (SCF) can be used as multiplication factor, and by using the SCF maximum stress can be predicted, thus it can predict the stress field around the local region. Thus the study of elastic stress field around discontinuous in geometry is very important for researchers and designers for safe- life of the components.

Peterson [1] studied the abrupt changes in geometry in components under static loading for the isotropic materials and reported its effect on design of machine component. The SCF for different composite materials are also presented by Shiau and Lee [2]. An analytical Stress concentration around irregular holes using complex variable methods are reported by Simhaand Mahapatra [3].

The analytical solution of infinite elastic plate with an circular hole andelliptic hole subjected to arbitrary biaxial loading was obtained by Gao [4]. Zirka *et al.* [5] have analyzed stress concentration around circular hole in a rectangular plate for orthotropic and isotropic plates under dynamic and static loading by using photo elastic method. Tafreshi [6] presented work on stress analysis of a series of thick, wide flatplates with oblique holes subjected to uniaxial tension. Amir R. Khamseh and Anthony M. Waas [7] experimentally investigated the failure mechanisms in fibrous laminated composite plates containing stress raisers, in the form of cutouts, under static biaxial planar compressive loading.Kalita et al. [8] studied the variation of deflection and induced stresses due to presence of central cutouts under transverse loading.Paul et al. [9] presented the deflection and bending moment in non-dimensional forms at different location of the plate by using a 9 node isoparametric element.

**Mathematical Formulation:**

**2.1 *Stress analysis in plates***

Stress analysis of an elastic body is usually three dimensional problem. But, most of the practical problems appear in the state of plane stress or plane strain. Stress analysis of three-dimensional bodies under plane stress or plane strain can be treated as two- dimensional problems. The solution of two-dimensional problems require the integration of the different equations of equilibrium together with the compatibility equations and boundary conditions. If body force is neglected, the equations to be satisfied are

$$\frac{\partial \sigma_x}{\partial x} + \frac{\partial \sigma_{xy}}{\partial y} = 0 \qquad (1)$$

$$\frac{\partial \sigma_y}{\partial y} + \frac{\partial \sigma_{xy}}{\partial x} = 0 \qquad (2)$$

$$\left(\frac{\partial^2}{\partial x^2} + \frac{\partial^2}{\partial y^2}\right)(\sigma_x + \sigma_y) = 0 \qquad (3)$$

Substitution of stress components by displacement components u and v into Eq. (1) to (3) makes Eq. (3) redundant and Eq. (1) and (2) transforms to

$$\frac{\partial^2 u}{\partial x^2} + \frac{(1-\nu)}{2}\left(\frac{\partial^2 u}{\partial y^2}\right) + \frac{(1+\nu)}{2}\left(\frac{\partial^2 v}{\partial x \partial y}\right) = 0 \qquad (4)$$

$$\frac{\partial^2 v}{\partial y^2} + \frac{(1-\nu)}{2}\left(\frac{\partial^2 v}{\partial x^2}\right) + \frac{(1+\nu)}{2}\left(\frac{\partial^2 u}{\partial x \partial y}\right) = 0 \qquad (5)$$

Now we need to find u and v from a two dimensional field satisfying the two partial differential Eq. (4) and (5).Instead of determining the two functions u and v the problem can be reduced to solving a single function $\psi(x,y)$, which can be determined by satisfying Eq. (4) and (5). The displacement potential function $\psi(x,y)$ can be defined as

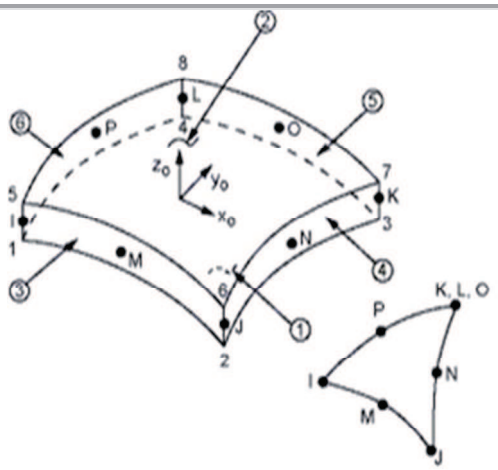


Fig.1: Shell element used in the analysis.

$$u = \frac{\partial^2 \psi}{\partial x \partial y} \qquad (6.1)$$

$$v = -\left[(1-\nu)\left(\frac{\partial^2 \psi}{\partial y^2}\right) + 2\left(\frac{\partial^2 \psi}{\partial x^2}\right)\right]/(1-\nu) \qquad (6.2)$$

By the above definitions the displacement components u and v satisfies Eq. (4) and the only condition reduced from Eq. (5) that the function ψ(x,y) has to satisfy is

$$\frac{\partial^4 \psi}{\partial x^4} + 2\left(\frac{\partial^4 \psi}{\partial x^2 \partial y^2}\right) + \frac{\partial^4 \psi}{\partial y^4} = 0 \qquad (7)$$

So, now the problem is to evaluate a single function Ψ(x,y) from the bi-harmonic Eq. (7), satisfying the boundary conditions specified at the boundary.

### *2.2 Boundary conditions*

#### *2.2.1 Fixed Edge Conditions*

If a plate is clamped at the boundary, then the deflection and the slope of the middle surface must vanish at the boundary. On a clamped edge parallel to the *y*axis at*x*= *a*, the boundary conditions are

$$w|_{x=a} = 0 \;\; ; \;\; \frac{\partial w}{\partial x}|_{x=a} = 0$$

At clamped edge parallel to the x axis at y = b the boundary conditions are

$$w|_{y=b} = 0 \;\; ; \;\; \frac{\partial w}{\partial y}|_{y=b} = 0$$

#### *2.2.2 Simply Supported Edge Conditions*

A plate boundary that is prevented from deflecting but free to rotate about a line along the boundary edge, such as a hinge, is defined as a simply supported edge. The conditions on a simply supported edge parallel to the y axis at x = a are

$$w|_{x=a} = 0$$

$$M_x|_{x=a} = -D\left(\frac{\partial^2 w}{\partial x^2} + \nu \frac{\partial^2 w}{\partial y^2}\right)_{x=a} = 0$$

Since the change of w with respect to the ycoordinate vanishes along this edge, the conditions become

$$w|_{x=a} = 0$$

$$\frac{\partial^2 w}{\partial x^2}|_{x=a} = 0$$

On a simply supported edge parallel to the x axis at y = b, the change of w with respect to the x coordinate vanishes, thus

$$w|_{y=b} = 0$$

$$M_y|_{y=b} = -D\left(\nu \frac{\partial^2 w}{\partial x^2} + \frac{\partial^2 w}{\partial y^2}\right)_{y=b} = 0$$

$$\frac{\partial^2 w}{\partial y^2}|_{y=b} = 0$$

**Methodology:** A thin rectangular plate of 1500mm x 1000mm x 2 mm (A x B x t) is considered for study. Square cutouts of side b are provided at the center. The cutout width (b) is varied from 100 mm to 500 mm i.e. ratio b/B of 0.1 to 0.5. For circular cutout study the radius (r) of the circularcutout at the center is varied from 50 mm to 250 mm thus varying the d/B ratio from 0.1 to 0.5. Two different materials are considered–an isotropic material (steel) with young's modulus (E) 200GPa and Poisson's ratio 0.3 and an orthotropic material (e-glass/epoxy) [10] with Ex, Ey, Ez, Gxy, Gyz, Gzx, μxy, μyz, μzx 3 GPa, 8.6GPa, 8.6GPa, 3.8GPa, 3.8GPa, 3.8GPa, 0.28, 0.28, 0.28 respectively. Equi-biaxial tensile stress of 10 MPa is applied at the edges. Three Different boundary conditions are considered.

*Plate A:* All sides are simply supported.

*Plate B:* Edges parallel to X-axis are fixed, other two are simply supported.

*Plate C:* Edges parallel to Y-axis are fixed, other two are simply supported.

An 8 node shell element, (specified as SHELL 281 in ANSYS) is used throughout the study (Fig.1). The element has eight nodes with six degrees of freedom at each node: translations in the x, y, and z axes, and rotations about the x, y, and z-axes (when using the membrane option, the element has translational degrees of freedom only). Thus each element has 48 degree of freedom in total. SHELL281 is well-suited for linear, large rotation, and large strain nonlinear applications.

It is a good practice and efficient way to exploit symmetry in FEM analysis whenever possible. Hence in this case only one quadrant of the plate is modelled and meshed. Mapped meshing is used to get finer mesh near the cutout periphery.

**Results and Discussion:** Each graph shows variation of a measured quantity (deflection or stress) with respect to cutout dimension (which is d/B for plate with circular cutout and b/B for plate with square

central hole). The markers (at data points) used in plots denote the geometry type of cutout. A, B and C in the plot indicate type of boundary condition used (as described in section 3 above). The data within the bracket in the graph indicate the type of cutout. For ex- A(Circular) means a rectangular plate with circular central cutout subjected to boundary conditions as detailed in section 3 as plate A i.e. all sides are simply supported.

**4. 1. *Deflection in X-direction:***

**4.1.1 *Isotropic material*:**

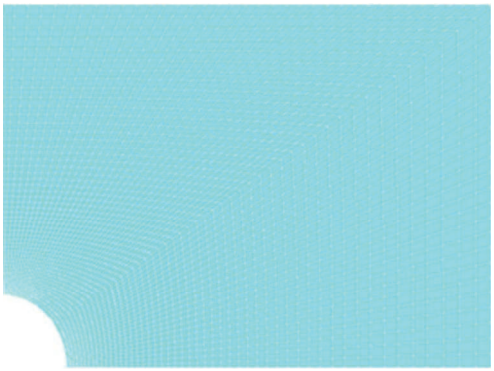

Fig. 2: A typical mesh used in the analysis

**4.1.2 *Orthotropic material*:** In the e-glass/epoxy plate though the $U_x/U_x^*$ variation pattern for all the three plates-A,B,C is similar to that of isotropic plates, a striking difference is seen in terms of magnitude of $U_x/U_x^*$ in Fig.4. At cutout ratio of 0.1 all the plates start atan $U_x/U_x^*$ ratio in between 2 to 3 whereas these was only around 1 for isotropic material. This means that in isotropic material the presence of a small cutout does not bring any significant change in the deflection pattern of the plate. But in an orthotropic material like e-glass/epoxy defection is 2 to 3 times more than a solid plate for a plate with small cutout (d/B or b/B= 0.1) and the deflection becomes significant when the cutout dimension is large in plate C. The $U_x/U_x^*$ increases manifold to 13.8 times for b/B=0.5 and 8.4 for d/B=0.5 for plate C.

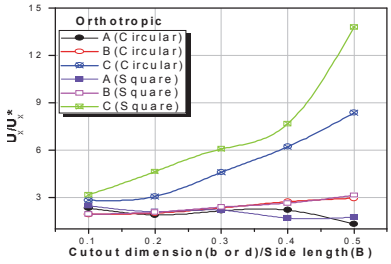


Fig.4: Ux/Ux* vs. Cutout dimension (orthotropic material )

Fig.3 shows the variation of $U_x/U_x^*$ with respect to cutout ratio is maximum in plate C. In plate A $U_x/U_x^*$ variation is almost same for both type of cutout, where it initiates at about 1 for d/B and b/B ratio of 0.1 and decrease to about 0.65 for cutout ratio 0.5. In plate B the $U_x/U_x^*$ is about 1.25 at cutout ratio 0.5 whereas it is more prominent in plate C. In plate C, at d/B=0.5 $U_x/U_x^*$ is 3.33 and 4.43 for b/B=0.5.Thus we see that deflection is more in case of plates with square cutouts.

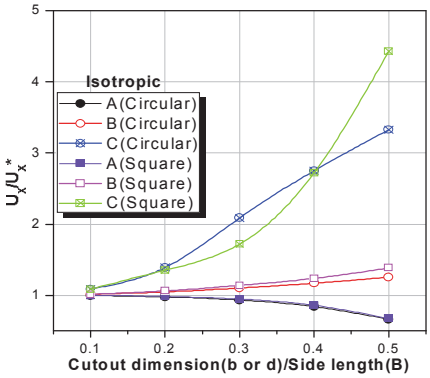


Fig.3: Ux/Ux* vs. Cutout dimension (Isotropic material)

**4. 2. *Deflection in Y-direction:***

**4.2.1 *Isotropic material*:**

Fig.5 shows the variation of $U_y/U_y^*$ with respect to cutout ratio is maximum in plate B for isotropic material. All the 3 plates show similar pattern-initially starts at 1 andthen deflection increases as the size of the cutout increases. In plate A, maximum$U_y/U_y^*$ is 3.1 for square cutout and 2.21 for circular cutout at cutout ratio 0.5. These plots for $U_y/U_y^*$ show that as cutout size increases the deflection in y-direction also increases.In plate B, max $U_y/U_y^*$ ratio is 3.8 and 2.5 for square and circular cutout respectively. In plate C, $U_y/U_y^*$ is 2.8 at b/B=0.5 and 2.1 at d/B=0.5. This variation is as per expectations since plate B is simply supported on edges parallel to y-direction.

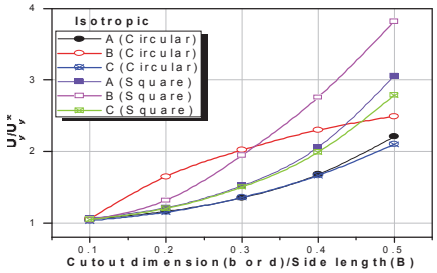


Fig.5:Uy/Uy* vs. Cutout dimension (Isotropic material)

**4.2.2 *Orthotropic material*:** The deflection in y-direction is maximum in plate B which is around 8 times higherfor a plate with large cutout as compared to a solid plate (without any cutouts). In Fig.6 Plate A and C shows similar variation of deflection, however plates with square cutout deflect slightly more than the ones with circular cutout. This might be due to the fact that a slightly larger amount of material is deducted in case of square cutout than in case of circular ones.

**4.3 *Distribution of $\sigma_x$ :***

**4.3.1 *Isotropic material*:**

Observation of variation of SCF for $\sigma_x$ with respect to cutout dimensions reveals that it is more prominent in plate C then in A and B as seen in Fig.7 in case of isotropic material. In all three plates increase of SCF for $\sigma_x$ is observed with increase in cutout ratio. In plate C for square cutout SCF for $\sigma_x$ is 3.04 at b/B=0.1 which increases to 4.93, for circular cutout it increases from 1.19 to 1.72. In plate A SCF for $\sigma_x$ increases from 2 to 2.5for square cutout and more or less constant for circular cutout.In plate B SCF for$\sigma_x$decreases from 1.4 at d/B=0.1 to 1 at d/B=0.5. However in case of square cutout it increases slightly 1.4 to 1.7 with increase in b/B from 0.1 to 0.5.

4.3.2 *Orthotropic material:* Fig.8 shows variation of SCF in orthotropic material for $\sigma_x$ which maximum in plate C for both cutout geometries.$\sigma_x$is seen to be minimum between cutout ratios 0.2 and 0.3 for all cases. With increase in cutout size the SCF for$\sigma_x$decreases until it reaches a minimum value and then again starts increasing with increase in cutout dimension.

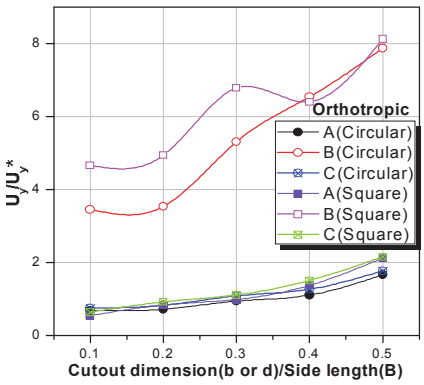


*Fig.6: Uy/Uy* vs. Cutout dimension (Orthotropic material)*

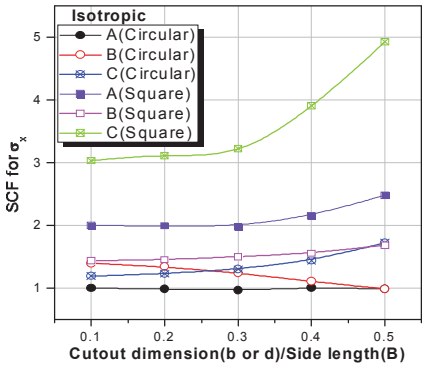


*Fig.7: SCF for σx vs. Cutout dimension (Isotropic material)*

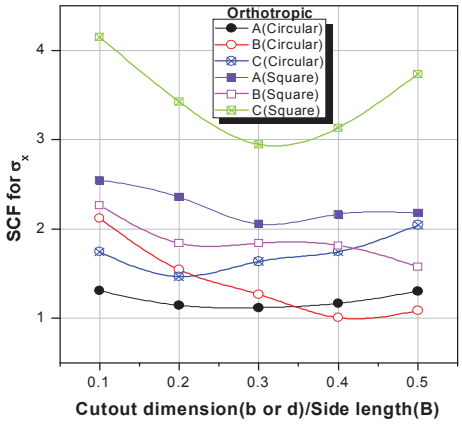


Fig.8: SCF for σx vs. Cutout dimension (Orthotropic material)

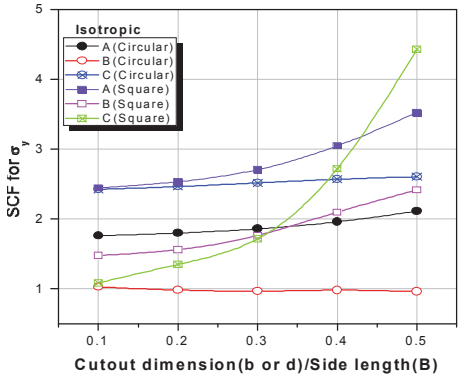


Fig.9: SCF for σy vs. Cutout dimension (Isotropic material)

**4. 4. *Distribution of $\sigma_y$ :***

**4.4.1 *Isotropic material*:**

Variation of SCF for $\sigma_y$ in isotropic material is prominent in plate C in which it increases from 1.1 at b/B=0.1 to 4.43 at b/B=0.5 and increases slightly for circular cutout between 2.4 to 2.6 (Fig. 9). The variation is maximum in all plates with square cutout as compared to the circular cutout ones. In plate A the SCF for $\sigma_y$increases from 1.76to 2.11 in circular cutout and from 2.45 to 3.5in square cutout. Plate B

shows the least SCF for $\sigma_y$, it ranges around 1 for the circular cutout but in square cutout increases from 1.4 to 2.4 for the isotropic material.

**4.4.2 *Orthotropic material:***

In orthotropic material SCF for $\sigma_y$ is maximum in plate B, prominent in plate C and least in plate A. In all the three plates with circular hole (Fig. 10) SCF remains almost constant throughout where it attains the least value for cutout size 0.2 or 0.3 and as we increase the cutout size the stress concentration increases. In plate B with square cutout SCF increases from 8.7 at b/B=0.1 to 9.6 at b/B=0.5 and is least at b/B=0.2.

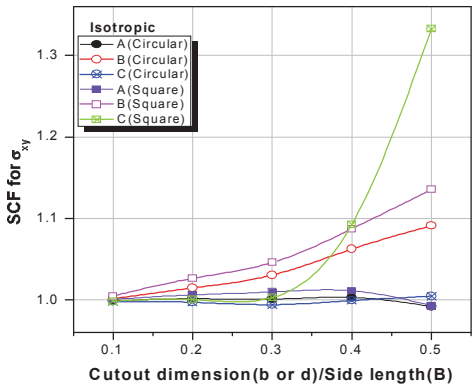


**Fig.11 SCF for σxy vs. Cutout dimension (Isotropic material)**

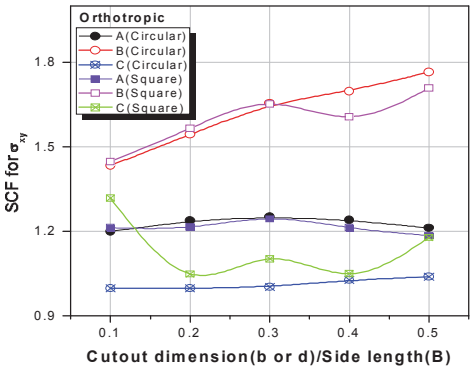


**Fig.12 SCF for σxy vs. Cutout dimension (Orthotropic material)**

**4. 5. *Distribution of $\sigma_{xy}$:*** 4.5.1 *Isotropic material*:

Fig.11 shows variation of SCF for $\sigma_{xy}$ for both type of cutouts is similar in isotropic material. Shear stress are more prominently present in plates with square cutouts. Plate C has a peak SCF of $\sigma_{xy}$ of 1.35. Apart from this particular case all other models reveal that concentration of shear stresses doesn't vary much and sticks around the 1.0 mark. Variation of shear stresses in all the cases even with increase in size of cutout is negligible.

**4.5.2 *Orthotropic material:***

In orthotropic material (Fig. 12) the variation of SCF for $\sigma_{xy}$ is maximum in plate B and significant for plate A and of least concern C. Maximum SCF for σxy is 1.76 and 1.71 for plate B with circular and square cutout respectively.

**Conclusion:** Variation of deflection in x-direction is maximum in plate C and is minimal in plate A for steel and e-glass/epoxy. Deflection in y direction is seen to be maximum for plate B for both materials. Max stress concentration is seen at hole periphery for plate C and B. In general, as compared to plate A stress is 52%- 60% less in plate B and 12%-18% less in plate C. Any Circular cutout replacing a square cutout shows a reduction in stress of about 5% in case of plate A to about2% in plate A. SCF for $\sigma_x$ and $\sigma_y$ varies most in plate C and least in plate A. The SCF in general in more in orthotropic plate as compared to isotropic plate. It is observed that SCF depends on elastic constants and hence differ from material to material. Hence we can conclude that SCF for $\sigma_x$ and $\sigma_y$ plays a critical role in design of plate C. Shear stresses are not of much prominence while designing thin plates under the action of biaxial stress. Also, a comparison with results of this study and reference 8 reveals that the stress concentration produced by a given cutout is not a unique number since it depends on the mode of loading.

**Acknowledgment:** The authors would like to gratefully acknowledge the various kinds of support received from friends and colleagues at Bengal Engineering and Science University, Shibpur, WB.

**References:**

1. R. E. Peterson, "Stress concentration design factors," New York: John Wiley and sons, 1966.
2. Le-Chung Shiau, George C. Lee, "Stress concentration around holes in composite laminates with variable fiber spacing," Volume 24, Issue 2, 1993, Pages 107-115
3. K. R. Y. Simha, S. S. Mohapatra, "Stress concentration around irregular holes using complex variable," Sadhana, Vol. 23, Part 4, 1998, pp. 393-412.
4. X. L. Gao, "A general solution of an infinite elastic plate with an elliptic hole under biaxial loading,"

Journal of Pressure Vessels and Piping, Vol. 67, 1996, pp. 95-104.
5. A. I. Zirka, M. P. Malezhik and I. S. Chernyshenko, "Stress distribution in an orthotropic plate with circular holes under impulsive loading," International Applied Mechanics, vol. 40, no. 2, 2004.
6. Tafreshi, "Numerical analysis of stresses at oblique holes in plates subjected to tension and bending,"Journal of strain analysis, vol. 30 no. 4, 1995, PP 317-323.
7. Amir R. Khamseh and Anthony M. Waas "Failure of Fibrous Composite Plates under StaticBiaxial Planar Loading."AIAA-94-1458-CP,American Institute of Aeronautics and Astronautics, Inc.
8. K. Kalita, and A. K. Banerjee, "Static Analysis of Isotropic & Orthotropic Plates with Central Cutout under Transverse Loading," Proceedings of NCRAME, NERIST, Nirjuli, 2013,pp.57-63.
9. Swagatam Paul, Kanak Kalita, Abir Dutta and S. Halder "Static analysis of rectangular plate with internal cut-out using finite element method," Proceedings of Indian Conference of Applied Mechanics, INCAM 2013, pp-144.
10. M. Daniel, and O. Ishai, "Engineering mechanics of composite materials," Oxford University Press, New York, USA, 1994.
11. K. Kalita, and S. Halder, "Stress Analysis of Cutout Plates," Proceedings of 58th congress of ISTAM, IIT Kharagpur, 2013.
12. R. B. Heywood, "Designing by Photo Elasticity," London: Chapman & Hall Ltd., 1952.

* * *

Dept. of Aerospace Engineering & Applied Mechanics,
Bengal Engineering and Science University, Shibpur, W.B.
kanakkalita02@gmail.com
Dept. of Aerospace Engineering & Applied Mechanics,
Bengal Engineering and Science University, Shibpur, W.B.